

Light-induced persistent electronic chirality in achiral molecules probed with transient absorption circular dichroism spectroscopy

Torsha Moitra*

*Hylleraas Centre for Quantum Molecular Sciences, Department of Chemistry,
UiT The Arctic University of Norway, 9037 Tromsø, Norway and
Department of Physical and Theoretical Chemistry,
Faculty of Natural Sciences, Comenius University, 81499 Bratislava, Slovakia*

Lukas Konecny

*Hylleraas Centre for Quantum Molecular Sciences, Department of Chemistry,
UiT The Arctic University of Norway, 9037 Tromsø, Norway
Department of Inorganic Chemistry, Faculty of Natural Sciences,
Comenius University, 81499 Bratislava, Slovakia and
Max Planck Institute for the Structure and Dynamics of Matter,
Center for Free Electron Laser Science, Luruper Chaussee 149, 22761 Hamburg, Germany*

Marius Kadek

*Hylleraas Centre for Quantum Molecular Sciences, Department of Chemistry,
UiT The Arctic University of Norway, 9037 Tromsø, Norway*

Ofer Neufeld

Technion Israel Institute of Technology, Faculty of Chemistry, Haifa 3200003, Israel

Angel Rubio†

*Max Planck Institute for the Structure and Dynamics of Matter,
Center for Free Electron Laser Science, Luruper Chaussee 149, 22761 Hamburg, Germany and
Initiative for Computational Catalysis (ICC), The Flatiron Institute,
162 Fifth Avenue, New York, New York 10010, USA*

Michal Repisky‡

*Department of Physical and Theoretical Chemistry, Faculty of Natural Sciences,
Comenius University, 81499 Bratislava, Slovakia and
Hylleraas Centre for Quantum Molecular Sciences, Department of Chemistry,
UiT The Arctic University of Norway, 9037 Tromsø, Norway*

(Dated: March 24, 2025)

Chiral systems exhibit unique properties traditionally linked to their asymmetric spatial arrangement. Recently, multiple laser pulses were shown to induce purely electronic chiral states without altering the nuclear configuration. Here we propose and numerically demonstrate a simpler realization of light-induced electronic chirality that is long-lived and occurs much before the onset of nuclear motion. Specifically, a single monochromatic circularly-polarized laser pulse can induce electronic chiral currents in an oriented achiral molecule. We analyze this effect with state-of-the-art ab-initio theory and connect the induced electronic chiral currents directly to induced magnetic dipole moments, which are detectable using attosecond transient absorption electronic circular dichroism spectroscopy. Our findings show that the chiral electronic wavepacket rapidly oscillates in handedness at frequencies corresponding to higher-order harmonics of the pump laser's carrier frequency, and the currents survive well after the laser pulse has turned off. Therefore, we propose a light-induced chiral molecular-current analogue to high harmonic generation, paving the way to attosecond transient chirality controlled by a single laser pulse. Such ultrafast chiral transients could enable emerging technologies such as enhanced spintronics, coherent control of chemical reactions, and more.

Chirality is a ubiquitous phenomenon observed in nature associated with the lack of mirror-image superimposability of systems ranging from macroscopic objects

to molecules [1, 2]. Traditionally, this concept is linked to geometric chirality, where the spatial arrangement of atoms within a molecule creates distinct left and right handedness. Light-induced *nuclear* dynamics operating on femtosecond timescales have shed light on intriguing phenomena where achiral molecules dynamically evolve into geometrically chiral structures via the loss of molecular symmetry [3–7]. However, it was only recently that

* torsha.moitra@uniba.sk

† angel.rubio@mpsd.mpg.de

‡ michal.repisky@uit.no

the concept of chirality has been realized without the intervention of nuclear degrees of freedom by pure *electronic* motion, giving rise to molecular light-induced electronic chirality [8, 9]. Closely intertwined with the concept of electronic chirality are ring currents, which are known to be induced by chiral light and light with orbital angular momentum [10]. Helical ring-currents can circulate through molecules [11–15] or outside of the molecule [16], breaking all spatial mirror/inversion symmetries of the system in 3D [17–19]. In previous works, symmetry breaking has been achieved by using two or more laser pulses, which is intuitively required in order to excite the molecule in a 3D spatial arrangement that breaks all relevant symmetries [4, 9, 20, 21].

Experimentally, ultrafast chiral states have been measured on the femtosecond timescale using time-resolved photoemission in atoms [13], and time-resolved photoelectron circular dichroism in chiral molecules [7, 8]. However, to our knowledge no work to date investigated pure attosecond chiral electron dynamics triggered by a single monochromatic light pulse without ionizing the molecule or breaking it apart. Such studies have been performed for magnetism in solids [22, 23], but it remains unclear if it is possible to connect attosecond circular-dichroic absorption spectra to chiral currents in molecules. Novel schemes for chiral state control could enable wide-ranging applications such as electronic switches [24], spintronics [25, 26], and phase transitions [27].

In this Letter, we study light-induced chirality originating from pure electron dynamics in structurally achiral furan molecule. We show that a single monochromatic circularly-polarized pulse is capable of inducing a chiral non-stationary electronic wavepacket in an oriented sample. This effect can be attributed to the induced ring currents generated by the pump pulse, which evolve dynamically in 3D. Interestingly, the current density is long-lived and the non-stationary chiral state does not instantaneously relax to an achiral state, therefore allowing its detection and monitoring and suggesting a way to generate chiral states that should survive up to few hundred femtoseconds before dephasing. We predict the spectroscopic signature of these chiral wavepackets based on the induced magnetic dipole moments by time-resolved electronic circular dichroism (TR-ECD), also referred to as transient absorption circular dichroism spectroscopy. These moments rapidly oscillate with frequencies corresponding not only to the pump laser’s carrier frequency, but also to its higher-order harmonics that survive long after the laser, and permits attosecond transient chiral states. Our work should therefore pave the way to attosecond chiral state manipulation and readout.

This study focuses on the furan molecule, which exhibits: (i) an achiral ground-state electronic configuration, (ii) a static electric dipole moment, which makes it orientable [28], and (iii) is frequently used in studies of other ultrafast phenomena [29–33]. Supplementary information extends this study to benzene and ani-

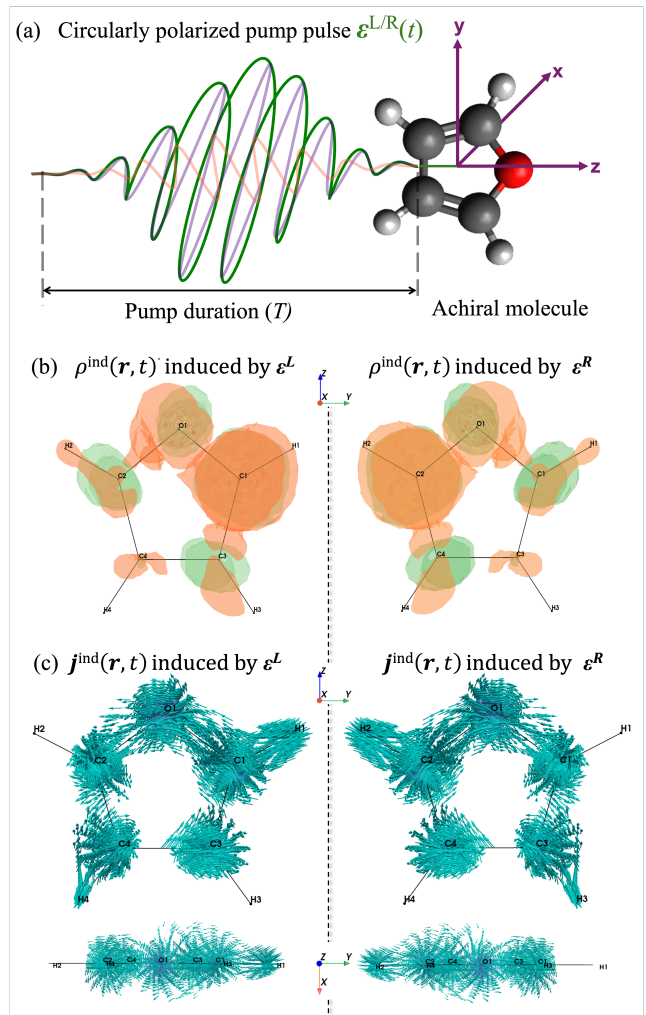


FIG. 1. (a) Schematic representation of a circularly-polarized pump pulse $\mathcal{E}^{L/R}(t)$ in green with xy plane of polarization and z propagation, interacting with the achiral furan molecule in yz plane. The chiral induced (b) electron charge density $\rho^{\text{ind}}(\mathbf{r}, t)$ and (c) current density $\mathbf{j}^{\text{ind}}(\mathbf{r}, t)$ generated by the circularly-polarized light at the end of the pump pulse ($t = T$). Gain and loss of charge density is shown by green and orange color surfaces with isovalue 0.005, respectively.

line molecules. Figure 1a illustrates our proposed setup for inducing chiral electron dynamics, where the furan molecule is oriented such that its static electric dipole moment is aligned with the direction of propagation of the CP light (along z). The molecule is initially pumped by a chiral, CP left (L) or right (R) laser pulse, whose electric field $\mathcal{E}^{L/R}(t)$ traces a circular trajectory in the xy -plane:

$$\mathcal{E}^{L/R}(t) = \mathcal{E}_0 g(t; t_0, T) [\cos(\omega_0(t - t_0))\mathbf{x} \mp \sin(\omega_0(t - t_0))\mathbf{y}]. \quad (1)$$

Here, $g(t; t_0, T)$ is a dimensionless Gaussian envelope centered at t_0 and duration T , while \mathcal{E}_0 and ω_0 are the amplitude and carrier frequency of the monochromatic light

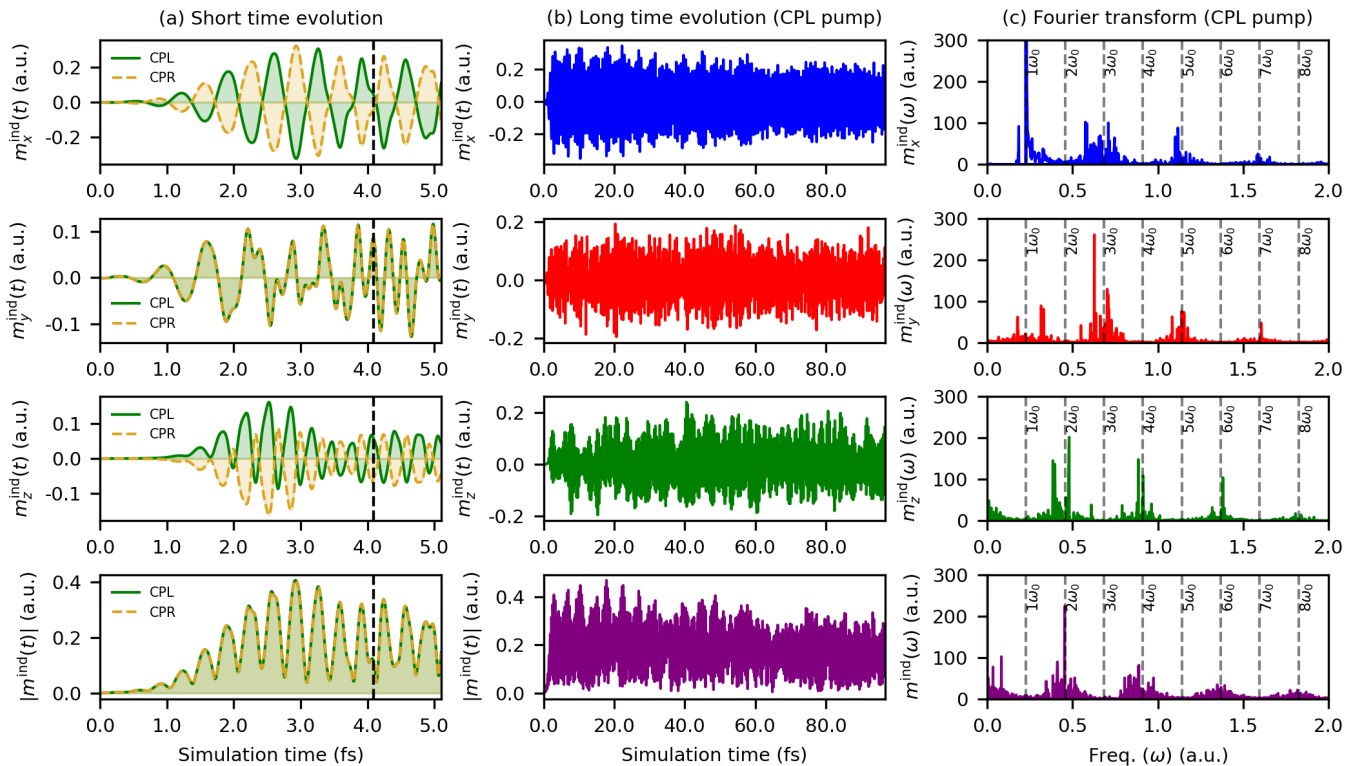


FIG. 2. Short time evolution (a) and long time evolution (b) of the magnitude ($|m^{\text{ind}}(t)|$) and components of the induced magnetic dipole moment $\mathbf{m}^{\text{ind}}(t) = (m_x^{\text{ind}}(t), m_y^{\text{ind}}(t), m_z^{\text{ind}}(t))$ by CPL and/or CPR pump pulses. The black dashed line in (a) at 4.09 fs marks the end of the pump pulse, after which the electronic wavepacket evolves freely. (c) Fourier transform of the induced magnetic moment obtained from the long time evolution in (b). The harmonic orders of the carrier frequency $\omega_0 = 0.223$ au are marked by dashed lines. Note that the simulation does not include dissipative processes.

pulse, respectively. Additional details about the pump pulse is given in Section S2. The carrier frequency was tuned to the first bright electronic transition at energy $\hbar\omega_0 = 0.223$ au = 6.07 eV, while T was set to 4.09 fs so that the pump pulse populates primarily the first excited state but also encompasses the second excited state at energy $\hbar\omega_1 = 0.294$ au = 7.99 eV. A pump pulse amplitude of $\mathcal{E}_0 = 0.03$ au corresponding to a peak intensity of 3.16×10^{13} W/cm² is used, which leads to about 3% ground state depopulation at the end of the pump, as shown in Section S3.

The interaction of an external pulse(s) with the molecule is described from first principles by real-time time-dependent density functional theory (RT-TDDFT) as implemented in the ReSpect program [34]. The electronic wavepacket is evolved in time-domain as per the Liouville-von Neumann (LvN) equation of motion,

$$i \frac{\partial \mathbf{D}(t)}{\partial t} = [\mathbf{F}(t), \mathbf{D}(t)] \quad (2)$$

where $\mathbf{D}(t)$ and $\mathbf{F}(t)$ are the time-dependent one-electron reduced density matrix and the Fock matrix, respectively. $\mathbf{D}(t)$ represents the state of the system, whereas $\mathbf{F}(t)$ characterizes the molecular system and its interaction with the external electric field within the dipole approx-

imation. Both matrices are represented in molecular orbitals (MOs), where each MO is expressed as a linear combination of Gaussian-type orbitals (GTOs). Here, we employed uncontracted aug-cc-pVTZ [35, 36] GTOs and PBE0 exchange-correlation functional [37]. We refer the reader to Section S1 for details on the RT-TDDFT methodology.

In order to get insights into ultrafast electron dynamics we compute the time-dependent induced electron charge (ρ^{ind}) and current (\mathbf{j}^{ind}) densities generated by the external pump pulse $\mathcal{E}^{\text{L/R}}(t)$. In our formalism, these quantities are defined over ground-state MOs (ϕ) as,

$$\rho^{\text{ind}}(\mathbf{r}, t) = \text{Tr}[\mathbf{D}^{\text{ind}}(t)\mathbf{\Omega}(\mathbf{r})] \quad (3)$$

$$\mathbf{j}_k^{\text{ind}}(\mathbf{r}, t) = \text{Tr}[\mathbf{D}^{\text{ind}}(t)\mathbf{J}_k(\mathbf{r})], \quad k \in x, y, z \quad (4)$$

where $\mathbf{\Omega}$ and \mathbf{J}_k are matrices of the charge density and current density operators

$$\Omega_{pq}(\mathbf{r}) = \phi_p^\dagger(\mathbf{r})\phi_q(\mathbf{r}) \quad (5)$$

$$\mathbf{J}_{k,pq}(\mathbf{r}) = -\frac{1}{2} \left(\phi_p^\dagger(\mathbf{r}) \{p_k \phi_q(\mathbf{r})\} + \{p_k \phi_p(\mathbf{r})\}^\dagger \phi_q(\mathbf{r}) \right). \quad (6)$$

The induced density matrix $\mathbf{D}^{\text{ind}}(t)$ is obtained as the difference between $\mathbf{D}(t)$ and the static ground-state $\mathbf{D}(0)$, which evolves on attosecond timescales.

The CPL and CPR pump pulses generate mirror-imaged induced charge and current densities, mimicking molecular enantiomers, as shown in Figs. 1b and 1c, respectively. The induced current density has both in-plane and out-of-plane contributions, as shown by the top view and side view in Fig. 1c. See supporting information video for time-evolution of the induced charge and current densities. Most importantly, the induced current density gives rise to a corresponding induced magnetic dipole moment in the system, evaluated as

$$\mathbf{m}^{\text{ind}}(t) = \frac{1}{2} \int d^3\mathbf{r} \mathbf{r} \times \mathbf{j}^{\text{ind}}(\mathbf{r}, t). \quad (7)$$

Figure 2a displays all components of the induced magnetic moment generated by CPL and CPR pump pulses in green and yellow, respectively. Notably, these induced moments persist well beyond the end of the pump pulse – indicated by the black dashed line in Fig. 2a – and exhibit periodic sign reversals. Furthermore, the overall magnitude of the induced magnetic moment $|\mathbf{m}^{\text{ind}}(t)|$ remains identical for both laser polarizations. A more detailed inspection of the individual components shows that $m_x^{\text{ind}}(t)$ and $m_z^{\text{ind}}(t)$ have opposite sign for CPL and CPR induced wavepacket, while $m_y^{\text{ind}}(t)$ has the same sign for both. This enantiomeric relationship is preserved during and after the pump pulse. Given the relative orientation of our pump laser with respect to the furan molecule, $m_x^{\text{ind}}(t)$ has the largest magnitude and can be attributed to the out-of-plane enantiomeric dynamics governed by π -bonding orbitals. A similar enantiomeric behavior is also observed for in-plane $m_z^{\text{ind}}(t)$ component, but with lower magnitude.

Fig. 2b presents the oscillations in the induced magnetic moment for the CPL induced wavepacket propagated for a long timescale of up to 100 fs. We would like to stress here that our simulations incorporate only pure electron dynamics, and have no external decoherence effects (nuclear motion, solvent effect, etc.), which would gain prominence at such large timescales. Nevertheless, even in this idealized scenario, the oscillations of the induced magnetic moment do not exhibit a single dominant frequency. A Fourier transform of the time-domain signal shows contribution from multiple harmonic orders of the laser pulse carrier frequency (ω_0), marked by dashed lines in Figure 2c. Therefore, it is impossible to define a single characteristic frequency for the flipping of the chiral state from one form to the other. The presence of higher harmonics also indicates that the induced electronic chirality opens up a route to coherent manipulation of ultrafast chiral states. The observation of multiple harmonic orders in the induced magnetic dipole moment suggests a light-matter mechanism analogous to high harmonic generation (HHG) [38–40], but where dynamics involved multiple harmonics even in much longer timescales, and in molecular magnetic moments rather than the typical dipole response that emits photons. Contrarily, the chiral-current harmonics do not cause light emission, but tune the speed with which the molecular handedness can

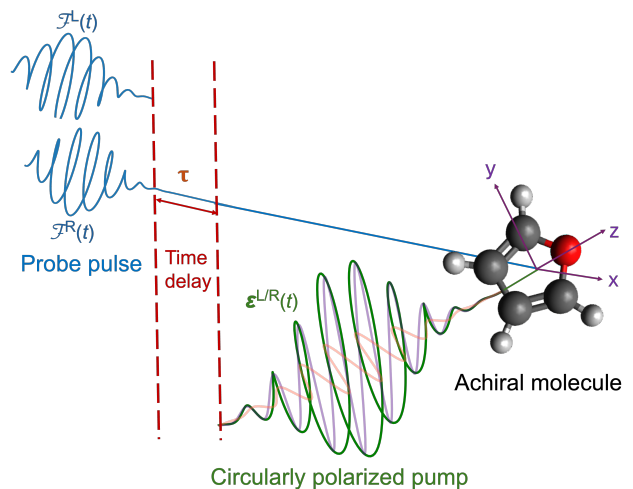


FIG. 3. Schematic representation of pump-probe setup for TR-ECD spectral simulation, where a probe pulse $\mathcal{F}^{L/R}(t)$ is applied at a time-delay of (τ) after the end of pump pulse $\mathcal{E}^{L/R}(t)$.

ultimately be controlled. Moreover, the observation that even harmonic orders appear in $m_y^{\text{ind}}(\omega)$, while odd harmonic orders are present in $m_x^{\text{ind}}(\omega)$ and $m_z^{\text{ind}}(\omega)$, suggests a symmetry-guided selection rule at play, possibly due to the parity of the chiral wavepacket [21]. The corresponding induced electric dipole moment and its Fourier transform is shown in Section S4. This rich harmonic content not only provides a spectral fingerprint of the underlying chiral dynamics and highlights the complex interplay between electronic motion and the system’s symmetry. Overall, these results suggest a route towards obtaining attosecond chiral transients even in the absence of using attosecond circularly-polarized pulses, which are very difficult to generate experimentally [41].

Having established the generation of chiral persistent currents with attosecond characteristics, let us discuss their potential observation. A standard approach to spectroscopically detect the induced magnetic dipole moment in structurally chiral systems is through electronic circular dichroism (ECD) absorption spectroscopy, which measures the differential absorption of left and right circularly polarized light [42–46]. We extend this technique to a typical pump-probe setup for obtaining time-resolved (TR-)ECD spectral signature; where the pump pulse, as discussed above, induces the electronic chirality in achiral oriented furan, while the probe pulse spectroscopically measures the induced chirality. This methodology forms the foundation of our proposed computational setup, as presented in Fig. 3.

Theoretically, the ECD spectral function is calculated in the weak-probe regime from the imaginary part of the Rosenfeld tensor $\beta(\omega)$ [42–44, 47, 48]. In the real-time TDDFT framework, this tensor can be obtained by the Fourier transformation of the time-dependent induced

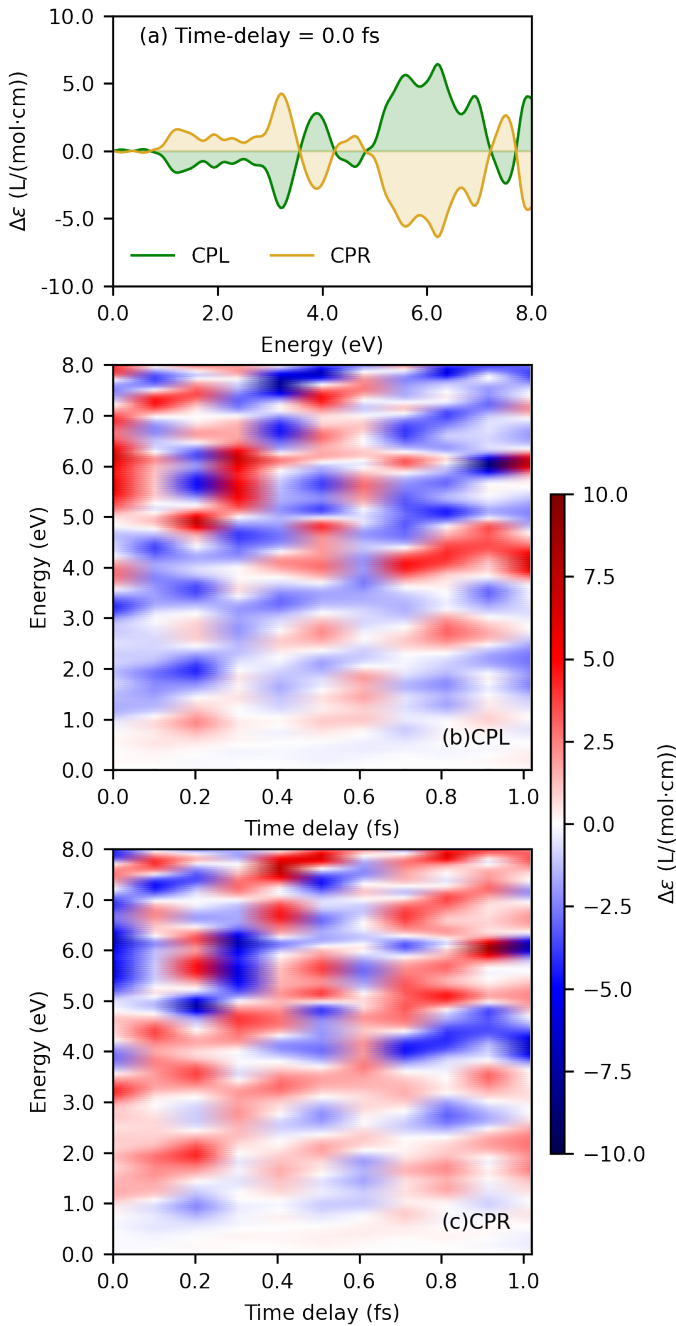


FIG. 4. Variation of time-resolved electronic circular dichroism (TR-ECD) as differential extinction coefficient ($\Delta\epsilon$), with pump-probe time delay (τ) induced by circularly polarized left CPL (a) and circularly polarized right CPR (b) pump pulses.

magnetic dipole moment recorded during time propagation [49–51]

$$\beta_{kj}(\omega) = \frac{i}{\omega \mathcal{F}_0 f_k} \int_{-\infty}^{\infty} dt m_j^{\text{ind}}(t) e^{i\omega t}, \quad k, j \in x, y, z. \quad (8)$$

In this approach, the probe pulse is represented by an analytical Dirac delta function, $\mathcal{F}(t) = \mathcal{F}_0 \mathbf{f} \delta(t - t_0)$, with

amplitude \mathcal{F}_0 , polarization vector \mathbf{f} , and initial time t_0 . We have extended this formalism to TR-ECD with the delta probe pulse applied at $t_0 = T + \tau$, where T is the pump pulse duration and τ is the time delay between pump and probe pulses. To isolate the response of the chiral electronic wavepacket to the probe pulse only, we subtract the magnetic dipole moment induced by the pump pulse, in analogy with transient absorption spectroscopy [52]. The essential theoretical background is discussed in details in Supplementary Information, Section S1.

The evolution of the chiral electronic wavepacket is monitored by varying the time-delay between pump and probe pulses, as shown in Fig. 4. TR-ECD spectra recorded immediately after the end of pump pulse displays mirror-image symmetry, as shown in Fig. 4a, indicating an enantiomeric relationship between the CPL and CPR induced wavepackets. Figures. 4b and 4c illustrate the full TR-ECD spectra as obtained with CPL (left) and CPR (right) light, respectively. The spectra are rich in information and the primary observations are as follows: (i) The mirror-image relationship between the CPL and CPR 2D signals is preserved over time. In other words, the helicity of the pump pulse induces an enantiomer-like relationship in the electronic wavepacket, and this relationship persists even during the rapid evolution of the chiral wavepacket. This observation is a direct consequence of the time-dependence of the induced magnetic moment shown in Fig. 2a, and the mirror relationship between CPR and CPL driving. (ii) The system exhibits chirality flips (sign reversal of TR-ECD spectral lines) generally on attosecond timescales observed on horizontal cuts in Figs. 4b and 4c. Notably, periods of these flips slightly vary for each energy window, likely connecting with various harmonics of the induced magnetic dipole moments presented in Fig. 2. Furthermore, we also investigated TR-ECD spectra of other oriented molecular systems, namely benzene and aniline. These results are delegated to the Supplementary Information, Section S6, and show similar chiral imprints induced by CPL and CPR pump pulses. These findings suggest that light-induced attosecond persistent electronic chirality in achiral systems is a robust and transferable phenomena.

In summary, our work explored the ultrafast chiral dynamics of oriented achiral molecules driven by a chiral pump pulse, demonstrating how electronic currents and their induced magnetic dipole moments encode a time-resolved chiral signature and persistent chiral molecular states. The induced magnetic dipole moment shows non-vanishing oscillations even after the end of the pulse, maintaining an enantiomer-like symmetry between CPL and CPR-induced electronic wavepackets. The time-resolved electronic circular dichroism spectra exhibit an imprint of this microscopic behaviors of the current densities and magnetic dipole moments, permitting experimental observation. We observe that the chiral response (both the magnetic dipole moment and the spectral function) does not oscillate with a characteristic frequency,

but rather emerges from a hierarchy of harmonic frequencies coherent with the pump laser. Unlike conventional HHG from time-dependent electric dipole moment, the observed harmonics in the magnetic dipole moment stem from bound electronic currents, presenting an alternative route for probing and controlling chiral states, down to attosecond timescales. This method provides a spectral fingerprint for chiral wavepacket evolution, offering a powerful tool to study attosecond chiral dynamics in non-ionized regimes. Looking forward, we believe that our results will motivate future studies in connected attosecond charge migration [53–56], systems that are usually studied with photoemission and photo-dissociation, potentially linking to energy transfer mechanisms. The induced chiral transients could also be employed for plethora of technological applications, from high selectivity ultrafast control of chemical reactions, to light-induced phase transitions [27], electronics [24], and spintronics [25, 26, 57]

ACKNOWLEDGEMENTS

We acknowledge the support received from the Research Council of Norway through a Centre of Excellence Grant (no. 262695), research grant (no. 315822), mobility grants (no. 301864 and no. 314814). T.M. acknowledges the support from the Marie Skłodowska-Curie individual postdoctoral fellowship (grant no. 101152113). In addition, M.R. acknowledges funding from the Euro-

pean Union’s Horizon 2020 research and innovation program under the Marie Skłodowska-Curie Grant Agreement no. 945478 (SASPRO2), the Slovak Research and Development Agency (grant no. APVV-22-0488), VEGA no. 1/0670/24, and the EU NextGenerationEU through the Recovery and Resilience Plan for Slovakia under the project No. 09I05-03-V02-00034. In addition, this work is supported by the Cluster of Excellence ‘CUI: Advanced Imaging of Matter’ of the Deutsche Forschungsgemeinschaft (DFG) - EXC 2056 - project ID 390715994. We acknowledge support from the Max Planck-New York City Center for Non-Equilibrium Quantum Phenomena. The Flatiron Institute is a division of the Simons Foundation. We thank Sigma2 - The National Infrastructure for High Performance Computing and Data Storage in Norway, grant no. NN14654K, and EuroHPC regular access grant no. EU-25-8 for the computational resources. We thank Stanislav Komorovsky for fruitful discussions about visualisation.

AUTHOR CONTRIBUTIONS

All authors conceptualized the project. T.M., L.K., M.K. and M.R. designed the algorithm and performed all necessary code implementations. T.M. performed all electronic structure calculations, curated data, and wrote the first draft of manuscript. All authors contributed to finalize the manuscript.

-
- [1] R. S. Cahn, C. Ingold, and V. Prelog, Specification of molecular chirality, *Angewandte Chemie International Edition in English* **5**, 385 (1966).
- [2] G. H. Wagnière, *On chirality and the universal asymmetry: reflections on image and mirror image* (John Wiley & Sons, 2007).
- [3] P. Changenet and F. Hache, Recent advances in the development of ultrafast electronic circular dichroism for probing the conformational dynamics of biomolecules in solution, *The European Physical Journal Special Topics* **232**, 2117 (2022).
- [4] D. Ayuso, A. F. Ordonez, and O. Smirnova, Ultrafast chirality: the road to efficient chiral measurements, *Physical Chemistry Chemical Physics* **24**, 26962 (2022).
- [5] M. Oppermann, F. Zinna, J. Lacour, and M. Chergui, Chiral control of spin-crossover dynamics in Fe(II) complexes, *Nature Chemistry* **14**, 739 (2022).
- [6] M. Oppermann, B. Bauer, T. Rossi, F. Zinna, J. Helbing, J. Lacour, and M. Chergui, Ultrafast broadband circular dichroism in the deep ultraviolet, *Optica*, 56 (2019).
- [7] S. Beaulieu, A. Comby, A. Clergerie, J. Caillat, D. Descamps, N. Dudovich, B. Fabre, R. Gêneaux, F. Légaré, S. Petit, *et al.*, Attosecond-resolved photoionization of chiral molecules, *Science* **358**, 1288 (2017).
- [8] V. Wanie, E. Bloch, E. P. Månsson, L. Colaizzi, S. Ryabchuk, K. Saraswathula, A. F. Ordonez, D. Ayuso, O. Smirnova, A. Trabattini, *et al.*, Capturing electron-driven chiral dynamics in uv-excited molecules, *Nature*, 1 (2024).
- [9] Y. Chen, D. Haase, J. Manz, H. Wang, and Y. Yang, From chiral laser pulses to femto- and attosecond electronic chirality flips in achiral molecules, *Nature Communications* **15**, 565 (2024).
- [10] K. A. Forbes and D. L. Andrews, Orbital angular momentum of twisted light: chirality and optical activity, *Journal of Physics: Photonics* **3**, 022007 (2021).
- [11] I. Barth, J. Manz, Y. Shigeta, and K. Yagi, Unidirectional electronic ring current driven by a few cycle circularly polarized laser pulse: quantum model simulations for Mg-porphyrin, *Journal of the American Chemical Society* **128**, 7043 (2006).
- [12] I. Barth and J. Manz, Electric ring currents in atomic orbitals and magnetic fields induced by short intense circularly polarized π laser pulses, *Physical Review A—Atomic, Molecular, and Optical Physics* **75**, 012510 (2007).
- [13] S. Eckart, M. Kunitski, M. Richter, A. Hartung, J. Rist, F. Trinter, K. Fehre, N. Schlott, K. Henrichs, L. P. H. Schmidt, *et al.*, Ultrafast preparation and detection of ring currents in single atoms, *Nature Physics* **14**, 701 (2018).
- [14] O. Neufeld and O. Cohen, Background-free measurement of ring currents by symmetry-breaking high-harmonic spectroscopy, *Physical Review Letters* **123**,

- 103202 (2019).
- [15] A. de Las Heras, F. P. Bonafé, C. Hernández-García, A. Rubio, and O. Neufeld, Tunable tesla-scale magnetic attosecond pulses through ring-current gating, *The Journal of Physical Chemistry Letters* **14**, 11160 (2023).
- [16] D. Pengel, S. Kerbstadt, D. Johannmeyer, L. Englert, T. Bayer, and M. Wollenhaupt, Electron vortices in femtosecond multiphoton ionization, *Physical Review Letters* **118**, 053003 (2017).
- [17] D. Pengel, S. Kerbstadt, L. Englert, T. Bayer, and M. Wollenhaupt, Control of three-dimensional electron vortices from femtosecond multiphoton ionization, *Physical Review A* **96**, 043426 (2017).
- [18] D. Ayuso, O. Neufeld, A. F. Ordonez, P. Decleva, G. Lerner, O. Cohen, M. Ivanov, and O. Smirnova, Synthetic chiral light for efficient control of chiral light-matter interaction, *Nature Photonics* **13**, 866 (2019).
- [19] N. Mayer, S. Patchkovskii, F. Morales, M. Ivanov, and O. Smirnova, Imprinting chirality on atoms using synthetic chiral light fields, *Physical Review Letters* **129**, 243201 (2022).
- [20] D. Habibović, K. R. Hamilton, O. Neufeld, and L. Rego, Emerging tailored light sources for studying chirality and symmetry, *Nature Reviews Physics* **6**, 663 (2024).
- [21] O. Neufeld, D. Podolsky, and O. Cohen, Floquet group theory and its application to selection rules in harmonic generation, *Nature Communications* **10**, 405 (2019).
- [22] F. Siegrist, J. A. Gessner, M. Ossiander, C. Denker, Y.-P. Chang, M. C. Schröder, A. Guggenmos, Y. Cui, J. Walowski, U. Martens, *et al.*, Light-wave dynamic control of magnetism, *Nature* **571**, 240 (2019).
- [23] O. Neufeld, N. Tancogne-Dejean, U. De Giovannini, H. Hübener, and A. Rubio, Attosecond magnetization dynamics in non-magnetic materials driven by intense femtosecond lasers, *NPJ Computational Materials* **9**, 39 (2023).
- [24] K. Morgenstern, Switching individual molecules by light and electrons: From isomerisation to chirality flip, *Progress in Surface Science* **86**, 115 (2011).
- [25] F. Evers, A. Aharony, N. Bar-Gill, O. Entin-Wohlman, P. Hedegård, O. Hod, P. Jelinek, G. Kamieniarz, M. Lemeshko, K. Michaeli, *et al.*, Theory of chirality induced spin selectivity: Progress and challenges, *Advanced Materials* **34**, 2106629 (2022).
- [26] R. Naaman and D. H. Waldeck, Chiral-induced spin selectivity effect, *The Journal of Physical Chemistry Letters* **3**, 2178 (2012).
- [27] H. K. Bisoyi and Q. Li, Light-driven liquid crystalline materials: from photo-induced phase transitions and property modulations to applications, *Chemical Reviews* **116**, 15089 (2016).
- [28] S. Fleischer, Y. Zhou, R. W. Field, and K. A. Nelson, Molecular orientation and alignment by intense single-cycle thz pulses, *Physical Review Letters* **107**, 163603 (2011).
- [29] T. Fuji, Y.-I. Suzuki, T. Horio, T. Suzuki, R. Mitrić, U. Werner, and V. Bonačić-Koutecký, Ultrafast photodynamics of furan, *The Journal of Chemical Physics* **133**, 234303 (2010).
- [30] Y. Liu, G. Knopp, C. Qin, and T. Gerber, Tracking ultrafast relaxation dynamics of furan by femtosecond photoelectron imaging, *Chemical Physics* **446**, 142 (2015).
- [31] W. Hua, S. Oesterling, J. D. Biggs, Y. Zhang, H. Ando, R. de Vivie-Riedle, B. P. Fingerhut, and S. Mukamel, Monitoring conical intersections in the ring opening of furan by attosecond stimulated x-ray raman spectroscopy, *Structural Dynamics* **3**, 023601 (2016).
- [32] S. Sun, B. Gu, H. Hu, L. Lu, D. Tang, V. Y. Chernyak, X. Li, and S. Mukamel, Direct probe of conical intersection photochemistry by time-resolved x-ray magnetic circular dichroism, *Journal of the American Chemical Society* **146**, 19863–19873 (2024).
- [33] R. Uenishi, A. Boyer, S. Karashima, A. Humeniuk, and T. Suzuki, Signatures of conical intersections in extreme ultraviolet photoelectron spectra of furan measured with 15 fs time resolution, *The Journal of Physical Chemistry Letters* **15**, 2222 (2024).
- [34] M. Repisky, S. Komorovsky, M. Kadek, L. Konecny, U. Ekström, E. Malkin, M. Kaupp, K. Ruud, O. L. Malkina, and V. G. Malkin, Respect: Relativistic spectroscopy dft program package, *The Journal of Chemical Physics* **152**, 184101 (2020).
- [35] T. H. Dunning Jr, Gaussian basis sets for use in correlated molecular calculations. i. the atoms boron through neon and hydrogen, *The Journal of Chemical Physics* **90**, 1007 (1989).
- [36] R. A. Kendall, T. H. Dunning, and R. J. Harrison, Electron affinities of the first-row atoms revisited. systematic basis sets and wave functions, *The Journal of Chemical Physics* **96**, 6796 (1992).
- [37] C. Adamo and V. Barone, Toward reliable density functional methods without adjustable parameters: The PBE0 model, *The Journal of Chemical Physics* **110**, 6158 (1999).
- [38] R. Cireasa, A. Boguslavskiy, B. Pons, M. Wong, D. Descamps, S. Petit, H. Ruf, N. Thiré, A. Ferré, J. Suarez, *et al.*, Probing molecular chirality on a sub-femtosecond timescale, *Nature Physics* **11**, 654 (2015).
- [39] O. Neufeld, D. Ayuso, P. Decleva, M. Y. Ivanov, O. Smirnova, and O. Cohen, Ultrasensitive chiral spectroscopy by dynamical symmetry breaking in high harmonic generation, *Physical Review X* **9**, 031002 (2019).
- [40] D. Ayuso, A. F. Ordonez, P. Decleva, M. Ivanov, and O. Smirnova, Strong chiral response in non-collinear high harmonic generation driven by purely electric-dipole interactions, *Optics Express* **30**, 4659 (2022).
- [41] P.-C. Huang, C. Hernández-García, J.-T. Huang, P.-Y. Huang, C.-H. Lu, L. Rego, D. D. Hickstein, J. L. Ellis, A. Jaron-Becker, A. Becker, *et al.*, Polarization control of isolated high-harmonic pulses, *Nature Photonics* **12**, 349 (2018).
- [42] L. D. Barron, *Molecular light scattering and optical activity* (Cambridge University Press, 2009).
- [43] A. E. Hansen and T. D. Bouman, Natural chiroptical spectroscopy: theory and computations, *Advances in Chemical Physics* , 545 (1980).
- [44] N. Berova, K. Nakanishi, and R. W. Woody, *Circular dichroism: principles and applications* (John Wiley & Sons, 2000).
- [45] I. Warnke and F. Furche, Circular dichroism: electronic, *WIREs Computational Molecular Science* **2**, 150 (2012).
- [46] S. S. Andrews and J. Tretton, Physical principles of circular dichroism, *Journal of Chemical Education* **97**, 4370 (2020).
- [47] L. Rosenfeld, Quantenmechanische theorie der natürlichen optischen aktivität von flüssigkeiten und gasen, *Zeitschrift für Physik* **52**, 161 (1929).

- [48] E. U. Condon, Theories of optical rotatory power, *Reviews of Modern Physics* **9**, 432 (1937).
- [49] D. Varsano, L. A. Espinosa-Leal, X. Andrade, M. A. Marques, R. Di Felice, and A. Rubio, Towards a gauge invariant method for molecular chiroptical properties in tddft, *Physical Chemistry Chemical Physics* **11**, 4481 (2009).
- [50] J. J. Goings and X. Li, An atomic orbital based real-time time-dependent density functional theory for computing electronic circular dichroism band spectra, *The Journal of Chemical Physics* **144**, 234102 (2016).
- [51] L. Konecny, M. Kadek, S. Komorovsky, K. Ruud, and M. Repisky, Resolution-of-identity accelerated relativistic two-and four-component electron dynamics approach to chiroptical spectroscopies, *The Journal of Chemical Physics* **149**, 204104 (2018).
- [52] T. Moitra, L. Konecny, M. Kadek, A. Rubio, and M. Repisky, Accurate relativistic real-time time-dependent density functional theory for valence and core attosecond transient absorption spectroscopy, *The Journal of Physical Chemistry Letters* **14**, 1714 (2023).
- [53] P. M. Kraus, B. Mignolet, D. Baykusheva, A. Ruppenyan, L. Horný, E. F. Penka, G. Grassi, O. I. Tolstikhin, J. Schneider, F. Jensen, *et al.*, Measurement and laser control of attosecond charge migration in ionized iodoacetylene, *Science* **350**, 790 (2015).
- [54] E. Goulielmakis, Z.-H. Loh, A. Wirth, R. Santra, N. Rohringer, V. S. Yakovlev, S. Zherebtsov, T. Pfeifer, A. M. Azzeer, M. F. Kling, *et al.*, Real-time observation of valence electron motion, *Nature* **466**, 739 (2010).
- [55] F. Calegari, D. Ayuso, A. Trabattoni, L. Belshaw, S. De Camillis, S. Anumula, F. Frassetto, L. Poletto, A. Palacios, P. Decleva, *et al.*, Ultrafast electron dynamics in phenylalanine initiated by attosecond pulses, *Science* **346**, 336 (2014).
- [56] F. Mauger, A. S. Folorunso, K. A. Hamer, C. Chandre, M. B. Gaarde, K. Lopata, and K. J. Schafer, Charge migration and attosecond solitons in conjugated organic molecules, *Physical Review Research* **4**, 013073 (2022).
- [57] R. Naaman, Y. Paltiel, and D. H. Waldeck, Chiral induced spin selectivity gives a new twist on spin-control in chemistry, *Accounts of Chemical Research* **53**, 2659 (2020).